

Ro-vibrational energy and thermodynamic properties of molecules subjected to Deng-Fan potential through an improved approximation

Debraj Nath *, Amlan K. Roy^{†‡}

May 20, 2022

Abstract

Accurate solution of the Schrödinger equation with Deng-Fan potential is presented by means of Nikiforov-Uvarov method. A modified Pekeris-type approximation is proposed for the centrifugal term, from a linear combination of the $r \rightarrow 0$ and $r \rightarrow r_e$ limits. It can potentially offer a series of approximations (depending on an adjustable parameter λ). The existing approximations in the literature can then be recovered in certain special cases. Its efficiency and feasibility is demonstrated by a critical comparison of eigenvalues produced at various λ 's for four molecules, *viz.*, H₂, LiH, HCl and CO. Analytical expressions are derived for energies, eigenfunctions and the thermodynamic properties such as vibrational mean free energy, vibrational free energy, vibrational entropy and vibrational specific heat. The effect of quantum correction on partition function and thermodynamic properties is discussed by including the correction up to 10th-order, for H₂ and LiH. The effect of λ parameter on these properties is also studied.

Key words: Deng-Fan potential, Nikiforov-Uvarov Method, Greene-type approximation, Pekeris-type approximation, ro-vibrational energy, vibrational partition function.

*Department of Mathematics, Vivekananda College, Thakurpukur, Kolkata-700063, India. Email: debrajn@gmail.com

†Department of Chemical Sciences, Indian Institute of Science Education and Research (IISER) Kolkata, Nadia, Mohanpur-741246, WB, India. Email: akroy@iiserkol.ac.in, akroy6k@gmail.com.

‡AKR dedicates this article to the loving memory of his kind-hearted teacher, late Prof. Hrishikesh Pradhan, P. K. College, Contai. Through his relentless, selfless service, he has influenced and inspired many chemists, over the years.

1 Introduction

A correct and proper representation of potential energy as a function of internuclear distance is an essential and indispensable tool for accurate understanding of structure and dynamics of a molecular system. An ideal potential energy function should show proper limiting behavior, i.e., $V(0) = \infty$ and approach a constant at infinite distance. Analytical eigenvalues and eigenfunctions are desirable, as they facilitate accurate estimation of transition frequencies and matrix elements. The oldest and arguably the most celebrated empirical Morse potential [1] was suggested almost ninety years ago. This widely used simple analytical functional has found valuable applications [2] in several branches in physics and chemistry including ro-vibrational states of diatomic molecules, adsorption of atoms/molecules on solid surface, deformation of cubic metals etc. The three-parameter exponential function is represented by,

$$U(r) = D_e [1 - \exp^{-\alpha(r-r_e)}]^2, \quad (1)$$

where D_e denotes dissociation energy, r_e corresponds to equilibrium internuclear distance and the Morse parameter α is defined in terms of force constant k_e as $\alpha = \sqrt{k_e/2D_e}$. Despite its remarkable success, the potential has a finite value, as internuclear distance approaches zero, and does not lead to the expected infinity nature. Thus when employed for the vibrational levels of diatomic molecule, the Morse oscillator shows considerable deviation from experimentally observed values. There has been many attempts to address these issues leading to a variety of proposals in the literature over the years. Some of the most prominent and notable ones are listed as follows: Kratzer [3, 4, 5], Rosen-Morse [6], Manning-Rosen [7, 8, 9, 10], Pöschl-Teller [11, 12, 13], Linnett [14], Hulthén [15, 16, 17, 18], Lippincott [19], shifted/Deng-Fan (DF) [20, 21, 22, 23, 24, 25], Tietz-Hua [26, 27, 28, 29], Schlöberg [30], Zavitsas [31], deformed Rosen-Morse [32, 33, 34], Woods-Saxon [35, 36, 37], pseudoharmonic [38, 39], Hajigeorgiou [40].

The current communication deals with the DF potential for diatomic molecules put forth about 70 years ago. This three-parameter function given in the following expression

$$V(r) = D_e \left(1 - \frac{b}{e^{ar} - 1}\right)^2, \quad b = e^{ar_e} - 1, \quad r \in (0, \infty), \quad (2)$$

has aroused considerable interest in last two decades. Here the three positive parameters D_e, r_e, a represent dissociation energy, equilibrium internuclear distance and radius of the potential well respectively. As internuclear distance approaches the limiting values zero and infinity, it offers a qualitatively correct asymptotic nature. This is also often referred as Generalized Morse potential due to its qualitative resemblance to Morse potential [41, 2]. This is also connected to another important diatomic potential due to Manning-Rosen [7].

Like the case of many other practical and realistic potentials, the relevant **Schrödinger equation with centrifugal term** can not be solved analytically for eigenvalues and eigenfunctions. This has led to the development of a number of **theoretical methodologies of approximation to the centrifugal term** in both non-relativistic and relativistic case. Some of the prominent ones may be mentioned. The authors in [41] have discussed the exact solvability problem via an $SO(2, 2)$ symmetry algebra. The eigenvalues and eigenfunctions for $\ell = 0$ states were studied by an algebraic method [42]. Approximate analytical solutions for rotating DF potential for arbitrary n, ℓ quantum numbers were given in terms of generalized hyper-geometric functions ${}_2F_1(a, b; c; z)$ [43]. An improved approximation scheme for the centrifugal term, along with a super-symmetric shape invariance approach was employed in [44]; analytical solution for Dirac equation has been presented with latter approach [45]. Solutions of Klein-Gordon equation with spinless particle for $\ell \neq 0$ states were considered in [46]. A Pekeris approximation for centrifugal term and a Nikiforov-Uvarov (NU) method was employed for Dirac, Klein-Gordon and Schrödinger equation [47, 48]. Some other methods include a numerical generalized pseudospectral (GPS) scheme [22], exact quantization rule [49, 23], a Feynman path integral formalism for D-dimensional problem [25], etc. A comparative analysis for the performance of Morse, Manning-Rosen, Schlöberg and DF potential in the context of diatomic molecules has been offered in [50].

Our objective in this communication is two-fold. At first, we present accurate eigenvalues and eigenfunctions of the DF potential by means of a simple novel approximation for the centrifugal term, within the framework of NU method. This is accomplished by taking a combination of approximations at $r \rightarrow 0$ and $r \rightarrow r_e$ limits. Its performance is critically analyzed by presenting the eigenvalues at various values of tunable parameter. These are compared with existing approximations available in the literature. The calculated ro-vibrational eigenvalues are offered for two representative diatomic molecules (H_2 , LiH). Both circular (s) as well as non-zero- ℓ states are obtained accurately. Then in the second stage, analytical expressions for vibrational partition function and related thermodynamic properties such as internal energy, free energy, entropy, specific heat capacity are derived. They are examined in terms of (i) temperature and (ii) the impact of quantum correction on these. The article is organized as follows. Section 2.1 provides the relevant details pertaining to the new approximation. The necessary expressions for eigenvalues and eigenfunctions within the NU method are detailed in Sec. 2.2. The associated energy spectrum is analyzed in Sec. 2.3. The expressions for thermodynamical quantities are given and discussed in Sec. 3 for a representative set of four diatomic molecules (H_2 , LiH, HCl and NO). Additionally the effect of quantum correction on the thermal quantities are discussed as well. Finally a few comments are made in Sec. 4.

2 The methodology

2.1 Analytical solutions of DF potential with centrifugal term within a new approximation

The time-independent non-relativistic Schrödinger equation for a diatomic molecule in presence of DF potential in Eq. (2), can be written as,

$$-\frac{\hbar^2}{2\mu}\nabla^2\psi(\mathbf{r}) + V(\mathbf{r})\psi(\mathbf{r}) = E\psi(\mathbf{r}), \quad (3)$$

where

$$\nabla^2 = \frac{1}{r^2}\frac{\partial}{\partial r}\left(r^2\frac{\partial}{\partial r}\right) + \frac{1}{r^2\sin\theta}\frac{\partial}{\partial\theta}\left(\sin\theta\frac{\partial}{\partial\theta}\right) + \frac{1}{r^2\sin^2\theta}\frac{\partial^2}{\partial\phi^2}, \quad (4)$$

with μ and \hbar denoting the reduced mass and Planck constant respectively. Let us define,

$$\psi(\mathbf{r}) = \frac{1}{\sqrt{2\pi}}\frac{R(r)}{r}Y_l^{m_l}(\theta)e^{im_l\phi}, \quad (5)$$

where $R(r)$ and $Y_l^{m_l}$ signify the usual radial and angular functions, while l, m_l represent the angular quantum numbers. Then one obtains the following radial Schrödinger equation,

$$\frac{d^2R(r)}{dr^2} + \left[\frac{2\mu}{\hbar^2}E - \frac{2\mu}{\hbar^2}V(r) - \frac{l(l+1)}{r^2}\right]R(r) = 0, \quad (6)$$

where $l(l+1)$ is the separation constant. Now one can expand (Pekeris-type approximation) $\frac{1}{r^2}$ as below,

$$\frac{1}{r^2} = \frac{f(x)}{r_e^2} = \frac{1}{r_e^2}\sum_{n=0}^{\infty}\frac{x^n}{n!}\left[\frac{d^n f(x)}{dx^n}\right]_{x=0} \approx \frac{1}{r_e^2}\sum_{n=0}^2\frac{x^n}{n!}\left[\frac{d^n f(x)}{dx^n}\right]_{x=0} + O(x^3), \quad (7)$$

where

$$f(x) = c_0 + \frac{c_1 s}{1-s} + \frac{c_2 s^2}{(1-s)^2}, \quad (8)$$

and

$$s = e^{-\alpha r}, r = r_e(1+x), \quad (9)$$

where x is a dimensionless variable. The coefficients c_0, c_1 and c_2 are dimensionless parameters.

In order to find these coefficients for non-zero l , one may express $\frac{1}{r^2}$ as [51, 27, 52],

$$\begin{aligned} \frac{1}{r^2} &= \frac{1}{r_e^2}\sum_{n=0}^{\infty}(-1)^n(n+1)x^n, \\ &\approx \frac{1}{r_e^2}(1-2x+3x^2+O(x^3)). \end{aligned} \quad (10)$$

Comparing the coefficients of Eq. (7) and Eq. (10), [52, 53, 25], one obtains,

$$\begin{aligned}
c_0 &= \frac{1}{u^2} [3 - 3u + u^2 + (2u - 6)s_e + (u + 3)s_e^2], \\
c_1 &= \frac{2}{s_e u^2} (1 - s_e)^2 ((3 + u)s_e + 2u - 3), \\
c_2 &= -\frac{1}{s_e^2 u^2} (1 - s_e)^3 ((3 + u)s_e + u - 3), \\
s_e &= e^{-u}, \quad u = \alpha r_e.
\end{aligned} \tag{11}$$

Let us now consider another approximation (Greene-type) [54, 23, 55, 21, 48] of the form,

$$\frac{1}{r^2} \approx \alpha^2 \left(\frac{1}{12} + \frac{s}{1-s} + \frac{s^2}{(1-s)^2} \right), \tag{12}$$

If we express $\alpha^2 \left(\frac{1}{12} + \frac{s}{1-s} + \frac{s^2}{(1-s)^2} \right)$ in the explicit form of r , then we obtain $\alpha^2 \left(\frac{1}{12} + \frac{s}{1-s} + \frac{s^2}{(1-s)^2} \right) \approx \frac{1}{r^2} + \alpha^2 \left(\frac{(\alpha r)^2}{240} - \frac{(\alpha r)^4}{6048} + \frac{(\alpha r)^6}{172800} + O((\alpha r)^8) \right)$. Hence it is better than Eq. (7), when $\alpha r \ll 1$. In the limiting case,

$$\frac{1}{r^2} = \lim_{\alpha \rightarrow 0} \alpha^2 \left(\frac{1}{12} + \frac{s}{1-s} + \frac{s^2}{(1-s)^2} \right). \tag{13}$$

Therefore, for a fixed α , Eq. (12) is a good approximation near $x = -1$ i.e., around $r = 0$ and Eq. (7) is good near $x = 0$ i.e., in region close to $r = r_e$. This prompts us to consider a linear combination of above two approximations, as in the following,

$$\frac{1}{r^2} \approx \alpha^2 \left(d_0(\lambda) + \frac{d_1(\lambda)s}{1-s} + \frac{d_2(\lambda)s^2}{(1-s)^2} \right), \tag{14}$$

where

$$d_0(\lambda) = \frac{\lambda}{12} + \frac{(1-\lambda)c_0}{u^2}, \quad d_1(\lambda) = \lambda + \frac{(1-\lambda)c_1}{u^2}, \quad d_2(\lambda) = \lambda + \frac{(1-\lambda)c_2}{u^2}. \tag{15}$$

From the above equation, it is observed that, $\lambda = 0$ implies Eq. (7) and $\lambda = 1$ signifies Eq. (12). Therefore, one can use Eq. (14) as a more general form of approximation for the centrifugal term $\frac{1}{r^2}$. As r increases, we can consider Eq. (14) for negative value of λ . In Fig. 1, the centrifugal term $\frac{1}{r^2}$ is plotted along with three approximations defined in Eqs. (7), (12) and (14), for H_2 . The panels (A), (B) refer to the corresponding functions in (-) ve and (+) ve domains of x . **For $0 \leq \lambda \leq 1$, the approximation of Eq. (14) is a convex combination of Eqs. (7) and (12), and the corresponding centrifugal term is a good approximation for $0 \leq r \leq r_e$. For negative values of λ , Eq. (14) is a good approximation to the centrifugal term for $r > r_e$, which is clear from Fig. 1(B).** It is noticed that the approximation defined in Eq. (14) is the best amongst them. This is generally found to be true for other molecules as well.

Using the transformation in Eq. (9) and approximation of Eq. (14) in Eq. (6) we obtain,

$$\frac{d^2 R}{ds^2} + \frac{1-s}{s(1-s)} \frac{dR}{ds} + \frac{-As^2 + Bs - C}{s^2(1-s)^2} R = 0, \tag{16}$$

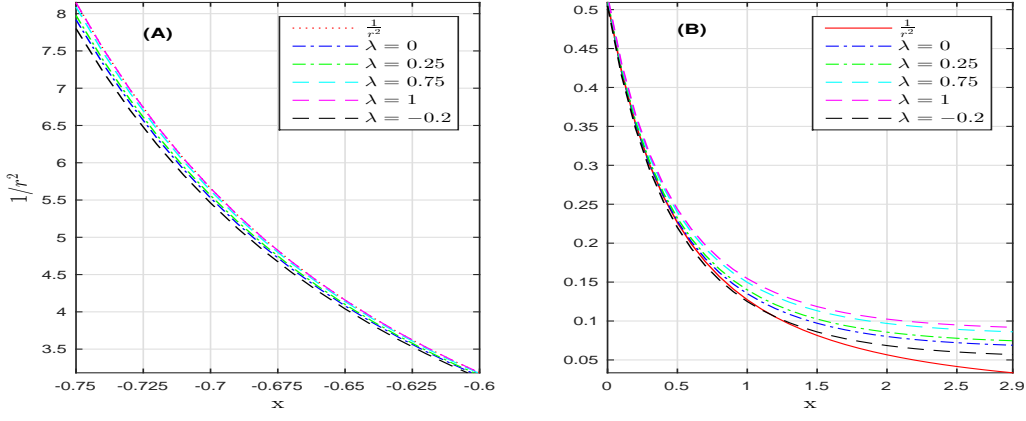


Figure 1: Plot of the centrifugal term $\frac{1}{r^2}$ and the three approximations given in Eqs. (7), (12) and (14) for H_2 molecule. The two situations $\lambda = 0, 1$ correspond to Eqs. (7) and (12) respectively. Panels (A), (B) refer to $(-)$ ve and $(+)$ ve regions of x .

where

$$\begin{aligned}
 A &= \bar{\varepsilon}^2 + 2b\beta^2 + b^2\beta^2 + \gamma(d_2 - d_1), \\
 B &= 2\bar{\varepsilon}^2 + 2b\beta^2 - \gamma d_1, \\
 C &= \bar{\varepsilon}^2, \\
 \bar{\varepsilon}^2 &= \beta^2 + \gamma d_0 - \varepsilon, \\
 \beta^2 &= \frac{2\mu D_e}{\alpha^2 \hbar^2}, \\
 \varepsilon &= \frac{2\mu E}{\alpha^2 \hbar^2}, \\
 \gamma &= l(l+1).
 \end{aligned} \tag{17}$$

Therefore, it reduces to an energy-dependent problem of a second-order differential equation. In the next subsection, we provide the solution of Eq. (16) by making use of NU method.

2.2 Nikiforov-Uvarov Method

One can compare Eq. (16) with the following Eq. [56, 57, 58, 21, 59],

$$\frac{d^2 R}{ds^2} + \frac{\tilde{\tau}(s)}{\sigma(s)} \frac{dR}{ds} + \frac{\tilde{\sigma}(s)}{\sigma^2(s)} R = 0, \tag{18}$$

where

$$\tilde{\tau}(s) = 1 - s, \quad \sigma(s) = s(1 - s), \quad \tilde{\sigma}(s) = -A s^2 + B s - C. \tag{19}$$

Let us consider the solution of Eq. (18) in following form,

$$R(s) = \phi(s)y(s). \tag{20}$$

Then one may obtain [56],

$$\sigma(s)y''(s) + \tau(s)y'(s) + \nu y(s) = 0, \quad (21)$$

and

$$\phi(s) = e^{\int \frac{\pi(s)}{\sigma(s)} ds}, \quad (22)$$

where

$$\begin{aligned} \pi(s) &= \frac{\sigma'(s) - \tilde{\tau}(s)}{2} \pm \sqrt{\left(\frac{\sigma'(s) - \tilde{\tau}(s)}{2}\right)^2 - \tilde{\sigma}(s) + k\sigma(s)}, \\ \tau(s) &= \tilde{\tau}(s) + 2\pi(s), \\ \nu &= k + \pi'(s). \end{aligned} \quad (23)$$

Here ν and k are real constants independent of s . Since $\pi(s)$ is a polynomial in s , $\left(\frac{\sigma'(s) - \tilde{\tau}(s)}{2}\right)^2 - \tilde{\sigma}(s) + k\sigma(s)$ is a square of a polynomial in s , and the solutions of Eq. (21) are given by,

$$y_n(s) = \frac{1}{\rho(s)} \frac{d^n}{ds^n} [\sigma^n(s)\rho(s)], \quad (24)$$

where

$$\rho(s) = [\sigma(s)]^{-1} e^{\int \frac{\tau(s)}{\sigma(s)} ds}. \quad (25)$$

Therefore, the corresponding eigenvalues are obtained from the relation,

$$\nu_n = -n\tau'(s) - \frac{n(n-1)}{2}\sigma''(s) = -n\tau'(s) + n(n-1), \quad n = 0, 1, 2, \dots \quad (26)$$

According to NU method, we obtain a pair of possible values of k , which are given by,

$$k_{\pm} = -\gamma d_1 + 2b\beta^2 \pm \bar{\varepsilon} \sqrt{4b^2\beta^2 + 4\gamma d_2 + 1}. \quad (27)$$

Now using Eq. (27), we obtain a set of possible values of $\pi(s)$ as,

$$\pi(s) = -\frac{s}{2} \pm \left\{ \begin{array}{l} \left(\bar{\varepsilon} - \frac{1}{2} \sqrt{4b^2\beta^2 + 4\gamma d_2 + 1} \right) s + \sqrt{C}, \quad k = k_+, \quad k_+ - B > 0 \\ \left(\bar{\varepsilon} + \frac{1}{2} \sqrt{4b^2\beta^2 + 4\gamma d_2 + 1} \right) s + \sqrt{C}, \quad k = k_-, \quad k_- - B > 0 \\ \left(\bar{\varepsilon} - \frac{1}{2} \sqrt{4b^2\beta^2 + 4\gamma d_2 + 1} \right) s - \sqrt{C}, \quad k = k_+, \quad k_+ - B < 0 \\ \left(\bar{\varepsilon} + \frac{1}{2} \sqrt{4b^2\beta^2 + 4\gamma d_2 + 1} \right) s - \sqrt{C}, \quad k = k_-, \quad k_- - B < 0 \end{array} \right\}. \quad (28)$$

Since $\tau'(s) < 0$, in this work, we have considered $k = k_-$, where $k_- - B < 0$ and select the following $\pi(s)$,

$$\pi(s) = -\frac{s}{2} - \left(\bar{\varepsilon} + \frac{1}{2} \sqrt{4b^2\beta^2 + 4\gamma d_2 + 1} \right) s + \sqrt{C}. \quad (29)$$

In that case, one gets,

$$\begin{aligned} \rho(s) &= s^{2\bar{\varepsilon}}(1-s)^{2L-1}, \\ \phi(s) &= s^{\bar{\varepsilon}}(1-s)^L, \end{aligned} \quad (30)$$

and

$$\begin{aligned} y_n &= s^{-2\bar{\varepsilon}}(1-s)^{-2L+1} \frac{d^n}{dx^n} [s^{n+2\bar{\varepsilon}}(1-s)^{n+2L-1}] = n! P_n^{(2\bar{\varepsilon}, 2L-1)}(1-2s), \\ &= \frac{\Gamma(n+2\bar{\varepsilon}+1)}{\Gamma(2\bar{\varepsilon}+1)} {}_2F_1(-n, n+2\bar{\varepsilon}+2L; 2\bar{\varepsilon}+1; s), \end{aligned} \quad (31)$$

where

$$L = \frac{1}{2} + \sqrt{\frac{1}{4} + b^2\beta^2 + \gamma d_2}. \quad (32)$$

The ro-vibrational energies E_{nl} of the DF potential can then be derived from the relation,

$$k + (2n+1)\pi'(s) = n^2. \quad (33)$$

Finally, the ro-vibrational energy spectrum can be secured from,

$$E_{nl} = d_4 - \frac{\alpha^2 \hbar^2}{2\mu} \left(\frac{d_3^2}{(n+L)^2} + \frac{(n+L)^2}{4} \right), \quad (34)$$

where

$$\begin{aligned} d_3 &= \frac{1}{2}(2+b)b\beta^2 + \frac{1}{2}\gamma(d_2 - d_1), \\ d_4 &= D_e + \frac{l(l+1)\hbar^2\alpha^2}{2\mu}d_0 + \frac{\alpha^2\hbar^2 d_3}{2\mu}. \end{aligned} \quad (35)$$

Therefore, the radial solution can be expressed as,

$$R_n(r) = N_{nl} s^{\bar{\varepsilon}}(1-s)^L {}_2F_1(-n, n+2\bar{\varepsilon}+2L; 2\bar{\varepsilon}+1; s), \quad (36)$$

where

$$N_{nl} = \left[\frac{2\bar{\varepsilon}\alpha(n+\bar{\varepsilon}+L)\Gamma(n+2\bar{\varepsilon}+1)\Gamma(n+2\bar{\varepsilon}+2L)}{n!(n+\bar{\varepsilon})\Gamma(n+2L)[\Gamma(2\bar{\varepsilon}+1)]^2} \right]^{\frac{1}{2}}, \quad (37)$$

is the normalization constant, derived from,

$$\int |\psi_{n,l,m_l}(\mathbf{r})|^2 d\mathbf{r} = 1, \quad d\mathbf{r} = r^2 \sin\theta dr d\theta d\phi. \quad (38)$$

Finally, the explicit form of eigenfunctions of DF potential can be written as,

$$\psi_{n,l,m_l}(\mathbf{r}) = \frac{N_{nl}}{\sqrt{2\pi}} \frac{R_n(r)}{r} Y_l^{m_l}(\theta) e^{im_l\phi}, \quad (39)$$

where

$$Y_l^{m_l}(\theta) = \left[\frac{(2l+1)(l-|m_l|)!}{2(l+|m_l|)!} \right]^{\frac{1}{2}} P_l^{|m_l|}(\cos\theta) e^{im_l\phi}. \quad (40)$$

2.3 Energy spectrum

To illustrate the effectiveness of our approximation, selected energies of DF potential are tabulated for two diatomic molecules, *viz.*, H₂ (homo-nuclear) and LiH (hetero-nuclear). In each case, 10 states are considered to cover a broad range. The parameters used are as follows: Bohr radius =

0.52917721092Å, Hartree energy = 27.21138505 eV, electron rest mass = $5.48577990946 \times 10^{-4}$ amu. Spectroscopic parameters for H₂ are: $D_e = 4.7446$ eV, $r_e = 0.7416$ Å, $\alpha = 1.9426$ Å⁻¹, $\mu = 0.50391$ amu, while for LiH, these are: $D_e = 2.515283695$ eV, $r_e = 1.5956$ Å, $\alpha = 1.1280$ Å⁻¹, $\mu = 0.8801221$ amu. In columns 3-7 of Table 1, our estimated energies from Eq. (34) are presented for five λ , namely $-0.25, 0, 0.75, 1$ and 1.25 respectively. A total of 10 states are given for each molecule for arbitrary n, l quantum numbers. It may be noted that, the energies were considered by means of super-symmetric quantum mechanics [53] and path integral approach [25]; these correspond to the case of $\lambda = 0$. On the other hand, the energies of NU method [48, 21], asymptotic iteration [55] and Hellmann-Feynman theorem [23] represent the $\lambda = 1$ case. For the so-called circular or $l = 0$ states, all the columns produce identical energies, which is expected from Eq. (14). But for $l \neq 0$ states, the energies in five columns differ from each other. It is noticed that the energies in 6th column (relating to $\lambda = 1$) completely reproduce those reported in [21].

These observations of Table 1 are graphically shown in Fig. 2, where the ro-vibrational energies of H₂ molecule are depicted for three representative states. The left and right panels give $D_e - E_{nl}$ and E_{nl} respectively; the state labels are provided in parentheses. Shifted energies are plotted as well, to ease the facilitation of comparison with select literature values. Five values of λ ranging from -0.5 to 1.5 including 0 , are considered. In each case, a line is generated. In the right panel, only reference energies of [21] are available, which are marked in blue color. For $\lambda = 1$, they fall on the straight line. In left panels, reference energies are available in scattered manner. But in any case, the available ones related to $\lambda = 1$ directly fall on the line as expected. The GPS energies of [22] remain slightly left off $\lambda = 0$, in $l \neq 0$ states in panels (B) and (F). However, this can happen as it is a purely numerical approach. A similar plot is also found for LiH molecule in Fig. 3. In this case, the reference results of [23] falls slightly right off $\lambda = 1$. This is presumably because of the differences in implementation of their method from ours; we use a NU scheme while they employed a Hellmann-Feynman approach. Note that in panel (C), the path-integral [25] and GPS [22] energies overlap. The latter results, like H₂, hover in the neighborhood of $\lambda = 0$. For a few other molecules, quite similar observations are made; hence they are omitted here.

3 Thermodynamical properties in DF potential

Now we move on to the derivation of thermodynamic quantities using the approximate solution of Sec. 2. The starting point for such calculations is the vibrational partition function. This can be constructed from a direct summation over all possible vibrational energy levels available to the

Table 1: Selected ro-vibrational energies (in eV) of H₂ and LiH, represented by DF potential. These correspond to five representative λ 's, indicated in parentheses. For more details, see text.

n	l	$E_{nl}(-0.25)$	$E_{nl}(0)$	$E_{nl}(0.75)$	$E_{nl}(1)^1$	$E_{nl}(1.25)$
H ₂						
0	0	0.349980221	0.349980221	0.349980221	0.349980221	0.349980221
1	0	0.996777053	0.996777053	0.996777053	0.996777053	0.996777053
1	1	1.009941717	1.010018022	1.010246935	1.010323238	1.010399541
2	0	1.580248366	1.580248366	1.580248366	1.580248366	1.580248366
2	1	1.592275484	1.592360547	1.592615732	1.592700793	1.592785853
2	2	1.616260599	1.616516418	1.617283848	1.617539648	1.617795443
5	0	2.986148433	2.986148433	2.986148433	2.986148433	2.986148433
5	5	3.118869192	3.120534519	3.12552957	3.127194276	3.128858827
5	10	3.452477485	3.458819802	3.477833081	3.484166293	3.490497236
5	15	3.935487614	3.950184048	3.994199652	4.008847068	4.023482314
LiH						
0	0	0.103334650	0.103334650	0.103334650	0.103334650	0.103334650
1	0	0.302005955	0.302005955	0.302005955	0.302005955	0.302005955
1	1	0.303739903	0.303759653	0.303818903	0.303838653	0.303858402
2	0	0.490685861	0.490685861	0.490685861	0.490685861	0.490685861
2	1	0.492346421	0.4923672887	0.492429891	0.492450759	0.492471626
2	2	0.495665829	0.495728464	0.495916365	0.495978997	0.496041629
5	0	0.999006401	0.999006401	0.999006401	0.999006401	0.999006401
5	5	1.020697858	1.021060955	1.022150163	1.022513206	1.022876235
5	10	1.077958316	1.079301598	1.083330322	1.084672857	1.086015205
5	15	1.169212076	1.1721857	1.181101026	1.184070957	1.187039967

¹These energies coincide with those from [21].

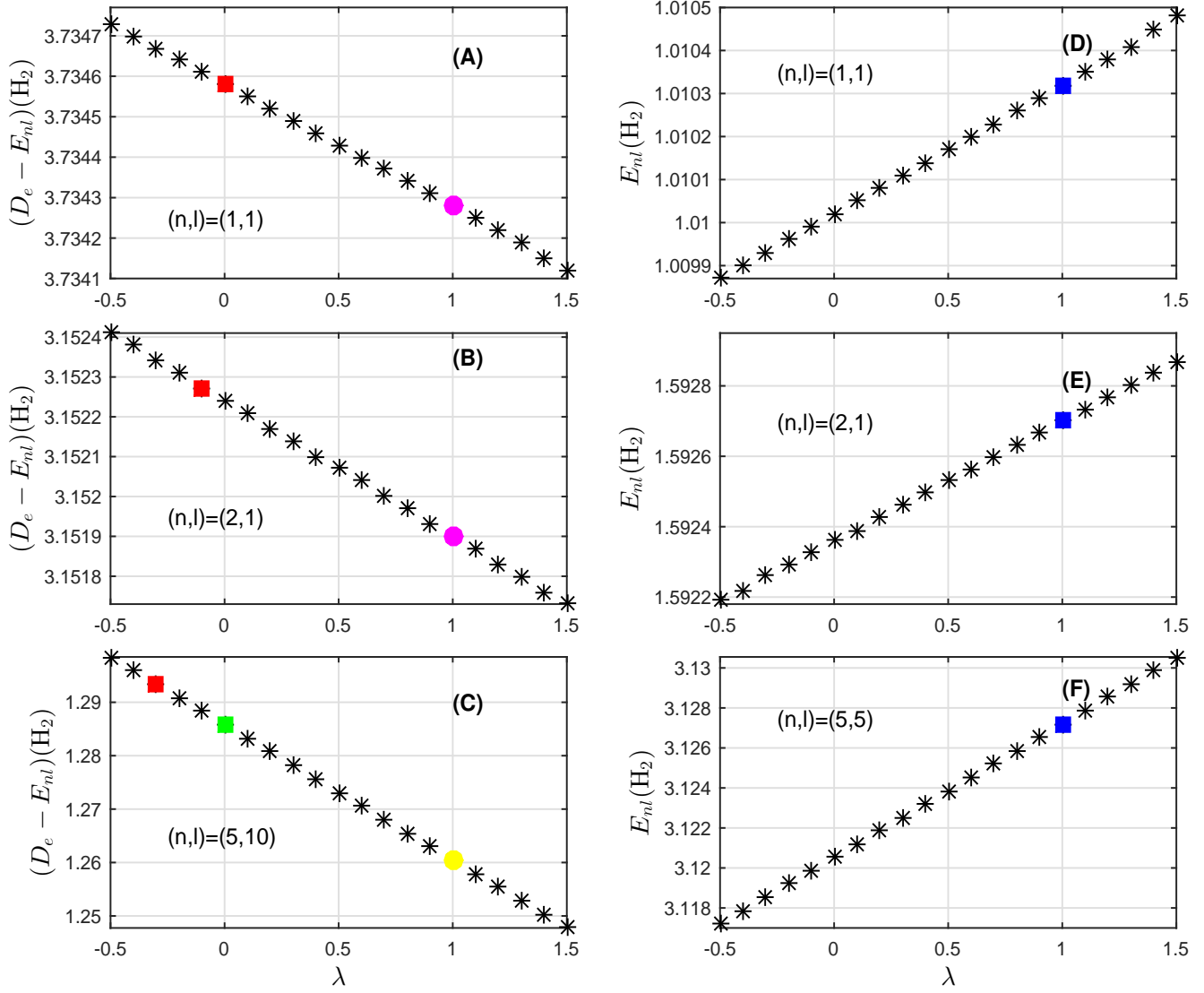


Figure 2: Plot of $(D_e - E_{nl})$ (left) and E_{nl} (right) of H_2 molecule in eV, against λ . The state indices are given inside the panels. The colored points show literature energies from various references as: red [22], magenta [23], green [25], yellow [55] and blue [21].

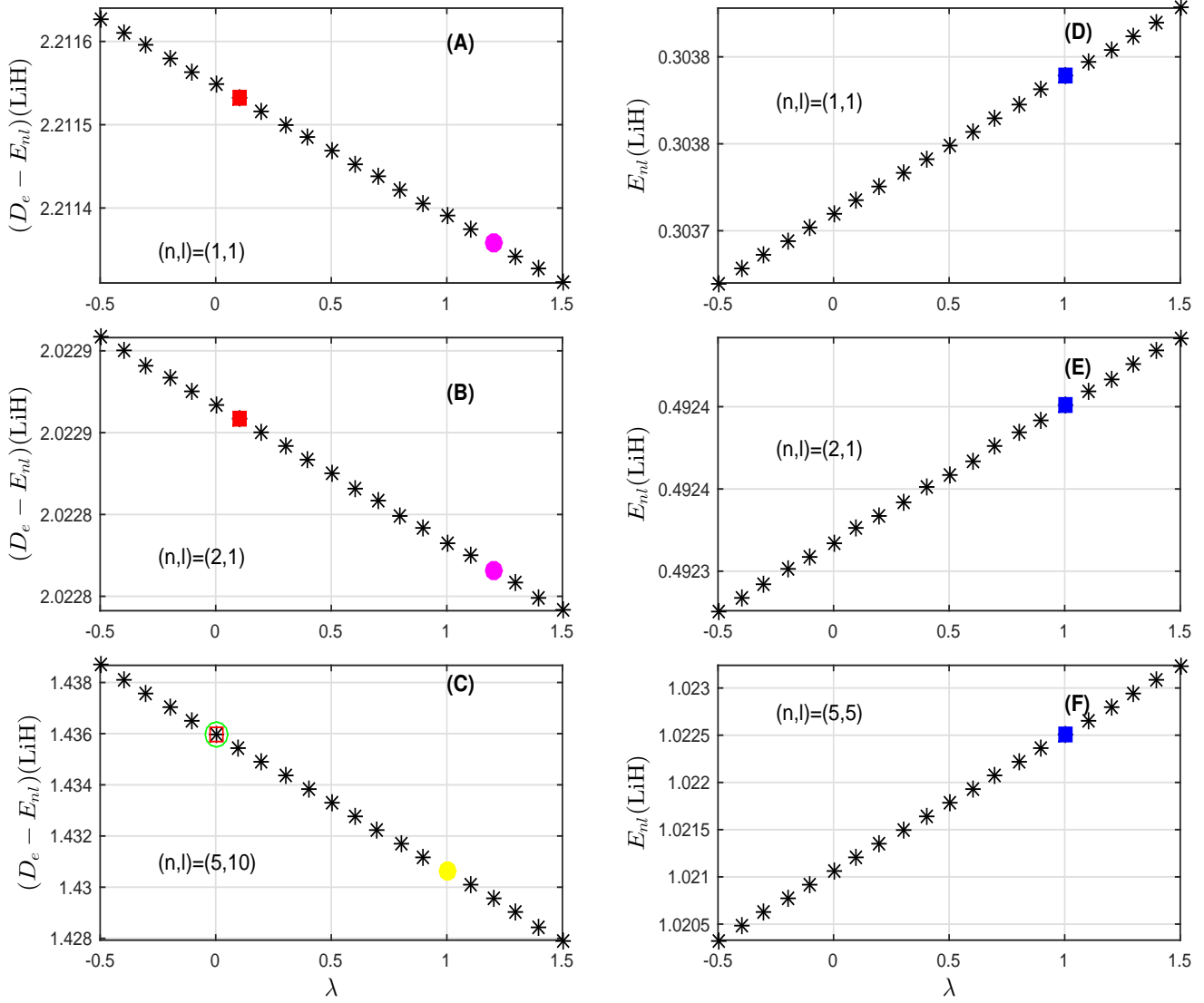


Figure 3: Plot of $(D_e - E_{nl})$ (left) and E_{nl} (right) of LiH molecule in eV, against λ . The state indices are given inside the panels. The colored points show literature energies from various references as: red [22], magenta [23], green [25], yellow [55] and blue [21].

system, namely,

$$Q(\beta) = \sum_{n=0}^{N_{max}} e^{-\beta E_n} \quad (41)$$

where $\beta = \frac{1}{kT}$, k denotes the Boltzmann constant and T is the temperature. For a finite summation with an upper bound N , the Poisson summation formula can be written as [60],

$$\sum_{n=0}^N f(n) = \frac{1}{2} [f(0) - f(N+1)] + \sum_{m=-\infty}^{\infty} \int_0^{N+1} f(x) e^{-i2\pi mx} dx. \quad (42)$$

Under the lowest-order approximation ($m = 0$), the above summation formula leads to [60],

$$\sum_{n=0}^N f(n) = \frac{1}{2} [f(0) - f(N+1)] + \int_0^{N+1} f(x) dx. \quad (43)$$

With the help of above relation, one can rewrite Eq. (41) in following form ('cl' stands for classical),

$$Z = Q_{cl}(\beta) = e^{-\beta d_4} \left\{ \frac{1}{2} e^{\frac{\alpha^2 \hbar^2 \beta}{2\mu} \left(\frac{d_3^2}{L^2} + \frac{L^2}{4} \right)} - \frac{1}{2} e^{\frac{\alpha^2 \hbar^2 \beta}{2\mu} \left(\frac{d_3^2}{(N_{max}+L)^2} + \frac{(N_{max}+L)^2}{4} \right)} + J_0^{(0)}(\beta) \right\} \quad (44)$$

where

$$J_m^{(j)}(\beta) = \int_L^{N_{max}+L} \left(\frac{d_3^2}{x^2} + \frac{x^2}{4} \right)^j \exp \left[\frac{\alpha^2 \hbar^2 \beta}{2\mu} \left(\frac{d_3^2}{x^2} + \frac{x^2}{4} \right) - i2\pi mx \right] dx \quad (45)$$

$$N_{max} = \left[\sqrt{2|d_3|} - L \right] + 1.$$

N_{max} is a (+)ve integer, $[x]$ denotes the integral part of x , and $[x] \leq x$. The energy is maximum at level $n = N_{max}$. The total partition function is a sum of classical ($m = 0$) and quantum corrected (Q_{QC}) contribution corresponding to ($m \neq 0$), i.e.,

$$Q_T(\beta) = Z(\beta) + Q_{QC}(\beta) \quad (46)$$

where

$$Q_{QC}(\beta) = \exp[-\beta d_4] \sum_{\substack{m=-N \\ m \neq 0}}^N \exp[i2\pi mL] J_m^{(0)}(\beta) \quad (47)$$

Now one can proceed for evaluation of quantities like internal energy ($U_T(\beta, N), U_{cl}(\beta)$), specific heat ($C_T(\beta, N), C_{cl}(\beta)$), free energy ($F_T(\beta, N), F_{cl}(\beta)$) and entropy ($S_T(\beta, N), S_{cl}(\beta)$) by using the usual expressions. The total partition function and corresponding thermal properties can be conveniently expressed in following simplified manner,

$$\begin{aligned} Q_T(\beta, N) &= H_0(\beta, N), & Z &= Q_{cl} = H_0(\beta, 0) \\ U_T(\beta, N) &= -\frac{1}{Q_T} \frac{\partial Q_T}{\partial \beta} = d_4 - \frac{H_1}{Q_T}, & U_{cl}(\beta) &= U_T(\beta, 0) \\ C_T(\beta, N) &= -k_\beta \beta^2 \frac{\partial U}{\partial \beta} = k_\beta \beta^2 \left(\frac{H_2}{Q_T} - \frac{H_1^2}{Q_T^2} \right), & C_{cl}(\beta) &= C_T(\beta, 0) \\ F_T(\beta, N) &= -k_\beta T \ln Q_T = -\frac{1}{\beta} \ln Q_T, & F_{cl}(\beta) &= F_T(\beta, 0) \\ S_T(\beta, N) &= k_\beta \ln Q_T + k_\beta T \frac{\partial \ln Q_T}{\partial T} = k_\beta \ln Q_T + k_\beta T \left(\frac{H_1}{Q_T} - d_4 \right), & S_{cl}(\beta) &= S_T(\beta, 0) \end{aligned} \quad (48)$$

where

$$\begin{aligned}
H_j(\beta, N) &= \left(\frac{\alpha^2 \hbar^2}{2\mu}\right)^j e^{-\beta d_4} \left[\frac{1}{2} \left(\frac{L^2}{4} + \frac{d_3^2}{L^2}\right)^j e^{\frac{\alpha^2 \hbar^2 \beta}{2\mu} \left(\frac{L^2}{4} + \frac{d_3^2}{L^2}\right)} - \frac{1}{2} \left(\frac{(N_{max}+L)^2}{4} + \frac{d_3^2}{(N_{max}+L)^2}\right)^j \right. \\
&\quad \left. e^{\frac{\alpha^2 \hbar^2 \beta}{2\mu} \left(\frac{(N_{max}+L)^2}{4} + \frac{d_3^2}{(N_{max}+L)^2}\right)} + \sum_{m=-N}^N \exp[i2\pi mL] J_m^{(j)}(\beta) \right], \quad (49) \\
\frac{\partial H_j(\beta, N)}{\partial \beta} &= H_{j+1}(\beta, N) - d_4 H_j(\beta, N).
\end{aligned}$$

The classical partition function and the corresponding classical thermal quantities are given in the right side.

Figure 4 depicts various calculated quantities, such as Z, U, C, F, S , for H_2 and LiH in left and right panels respectively, with respect to β , in atomic unit. The classical partition function $Q_{cl}(\beta)$ along with its 5th-order quantum correction, $Q_T(\beta, 5)$ and 10th order, $Q_T(\beta, 10)$. All these calculations are performed with energies corresponding to $\lambda = -0.25$ in Eq. (34), while N_{max} for a particular molecule is given in Eq. (45). They all monotonically increase (decrease) with temperature (β). The differences in Z from the classical and quantum-corrected counterparts are shown in the onset panels in red and blue colors for 5th and 10th orders respectively. It is seen that, the two differences tend to converge in the low- β region and show some deviations for large β . In other words, the $m \neq 0$ terms in Eq. (42) should be taken in to consideration for vibrational partition function in the low temperature region. Next, panels (C), (D) illustrate the changes in vibrational mean energies in H_2 and LiH , along with the effects of quantum correction inside. In both cases, U fall off with β starting from a certain positive value at $\beta \rightarrow 0$, i.e., it grows monotonically with T. There is a slight difference in the nature of plots for two molecules; for LiH it is almost straight, but for H_2 , one finds a minor bent. However, like the plots in (A), (B), the differences in this occasion also remain small; and as β progresses, the 5th and 10th order corrections show some variations (somehow rather more pronounced for LiH). Slight fluctuation is observed in case of LiH . For H_2 , the curve shows some flattish character at low T. The dependence of vibrational specific heat U for the two molecules are now recorded in segments (E) and (F). At first it gradually increases with β to reach a maximum and thereafter tends to decline. In both molecules, the quantum corrections make significant impacts in the behavior of C in low T region, with vigorous fluctuations in the corresponding differences. The vibrational free energies F are produced in (G) and (H), which show a sharp rise at low β to reach a maximum value, and then approaching a constant with further growth in β . The differences in classical and quantum corrections in this case appear to be rather small, while the 5th and 10th order results remain in harmony with each other. The last two panels (I) and (J) depict the analogous plots for vibrational entropy. After attaining a sharp maximum at lower β , for both molecules it monotonically decay. Similar plots are given in Fig. (5) for HCl and CO in left and right sides. The

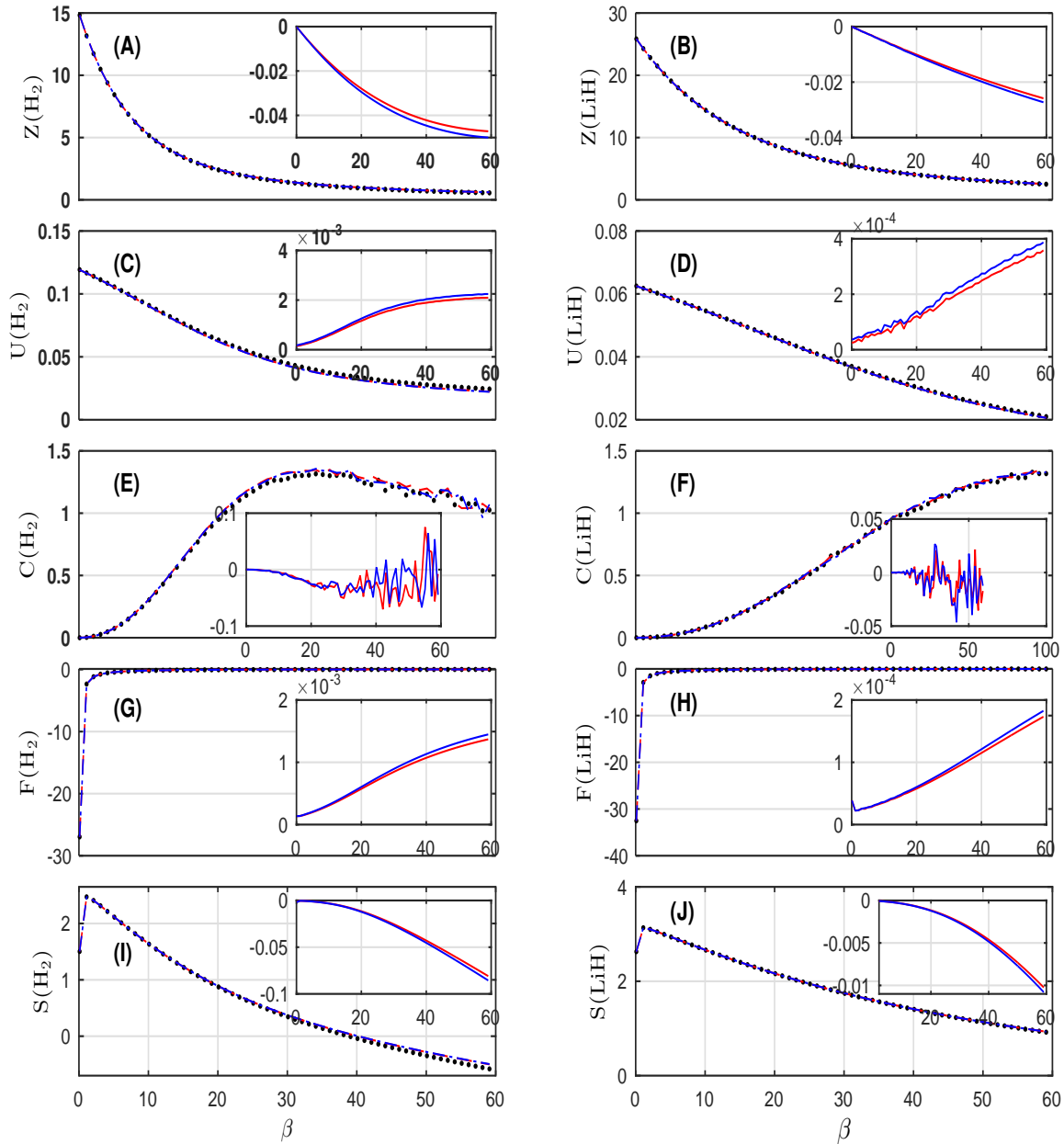


Figure 4: Plot of classical and N -corrected thermal properties as functions of β , for H_2 (left) and LiH (right), in atomic unit. The classical quantities are shown in black, while the effect of quantum correction on thermal properties are shown for $N = 5$ (red) and $N = 10$ (blue). Inset of each figure shows the difference between classical and quantum corrected thermal properties. Insets of (A), (B) represent $(Q_{cl}(\beta) - Q_T(\beta, 5))$ (red) and $(Q_{cl}(\beta) - Q_T(\beta, 10))$ (blue) for H_2 and LiH . In a similar manner, other quantities are depicted as follows: (C),(D): internal energies, (E),(F): specific heats, (G),(H): free energies, and (I),(J): entropies.

vibrational partition functions drop sharply in low β region in contrast to the previous figure. The differences in Z from classical to N th corrected quantity apparently become more significant in CO. The features in U plots remain very similar. One notices much stronger deviations from classically and corrected C in case of HCl amongst all the four molecules considered in these two figures. Also for CO, the variation of C differs from the rest of molecules. The F plots in these molecules resemble those of previous figure. The vibrational entropies very sharply decay at low β and thereafter remains practically constant throughout the whole range of β studied.

Finally, to estimate the role of parameter λ on the thermodynamical quantities, Fig. (6) portrays the relevant differences in Z, U, C, F, S for H_2 and LiH molecules in left and right panels respectively. In this case we employ classical partition functions for all the calculations. In each case the deviations of corresponding quantities are calculated with respect to $\lambda = 0$. Five λ are chosen for this, *viz.*, $-0.25, 0.25, 0.75, 1$ and 1.25 . It is observed that, the differences are in general, not very significant. One finds the impact to be small through out the whole range of β undertaken here.

4 Conclusion

A simple useful approximation for the centrifugal term is proposed for solution of Schrödinger equation in certain potentials through an amalgamation of $r \rightarrow 0$ and $r \rightarrow r_e$ **limits**. This is applied to derive expressions for eigenvalues and eigenfunctions in Deng-Fan molecular potential. The method offers accurate results ro-vibrational energies for $l = 0$ as well as $l \neq 0$ states. This is tested for four molecules (H_2, LiH, HCl, CO) through a comparison with other existing results in the literature. The effect of λ on energies is analyzed. These are now utilized to calculate the vibrational partition function and thermodynamic properties such as internal energy, specific heat, free energy and entropy in two representative diatomic molecules (H_2, LiH). The impact of quantum correction as well as λ on these properties is discussed by considering the quantum correction up to 10th order, which suffices our purpose. The method can be easily extended to other potentials (both central and non-central) including molecular potentials, such as Manning-Rosen, Pöschl-Teller, Hülthen, etc. It would be worthwhile to verify its applicability and performance in these cases, some of which may be taken up in future.

5 Acknowledgement

AKR gratefully acknowledges financial support from MATRICS, DST-SERB, New Delhi (sanction order: MTR/2019/000012).

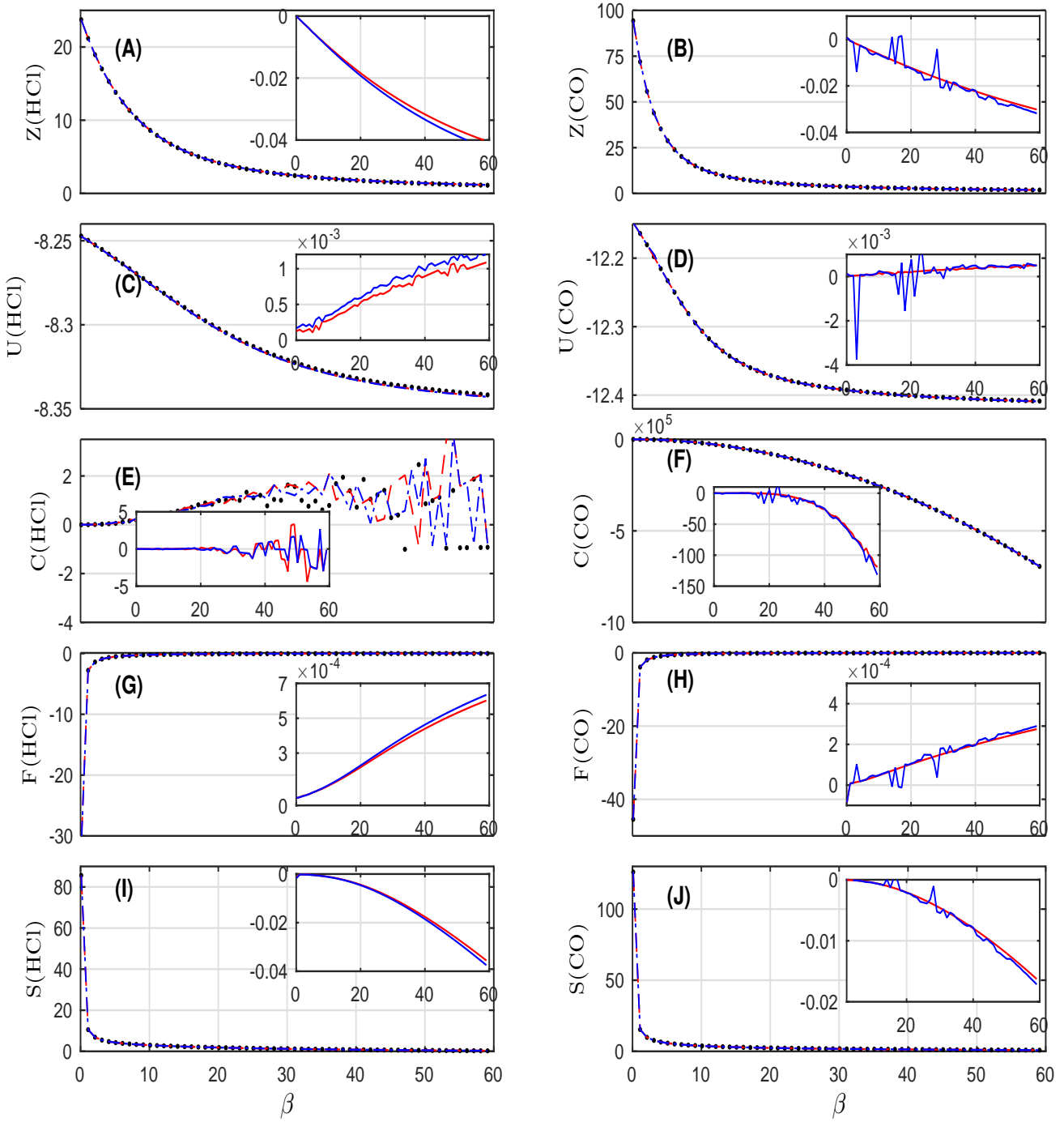


Figure 5: Plots of Z, U, C, F, S as functions of β , for HCl (left) and CO (right), in atomic unit, as in Fig. (4).

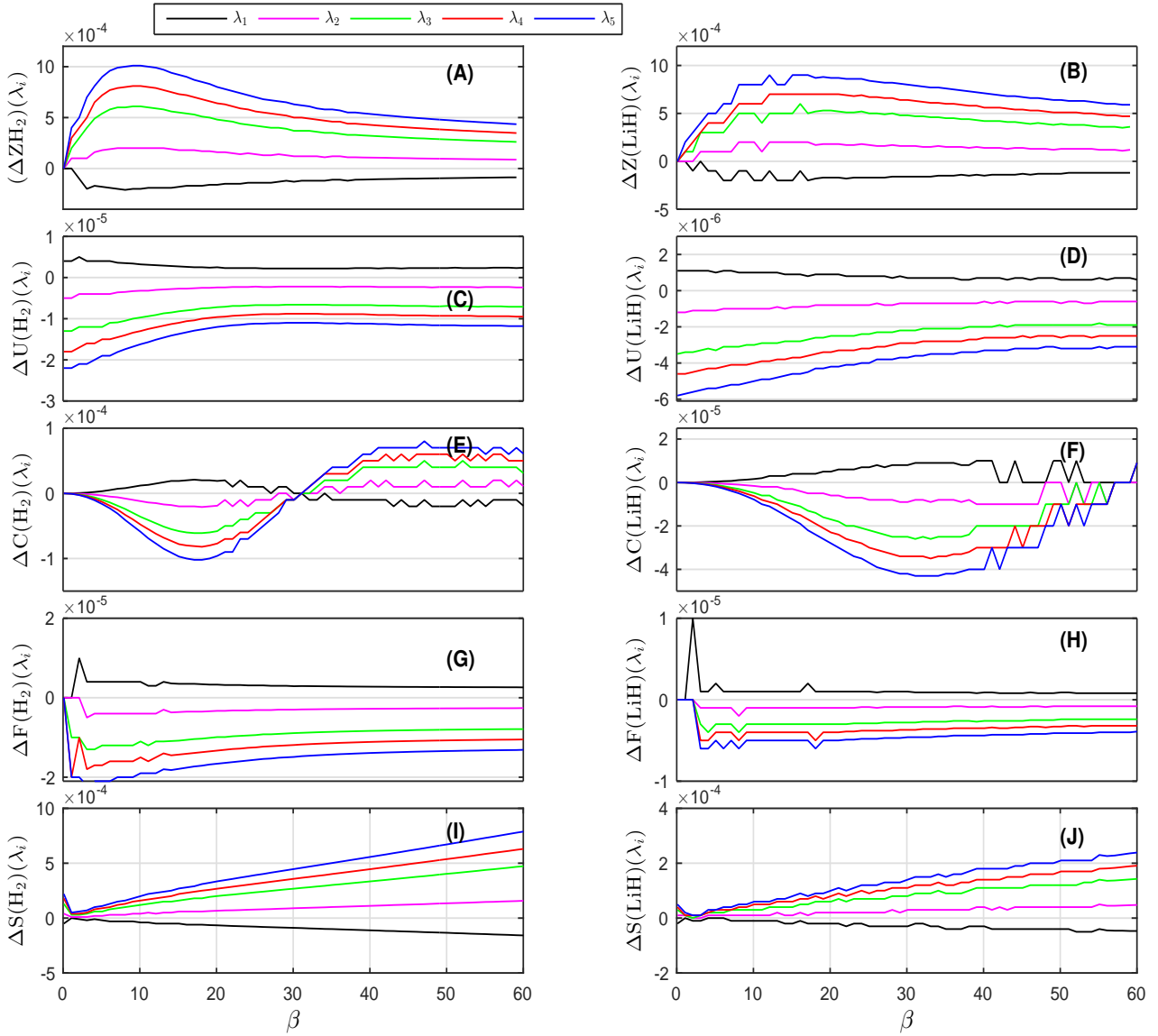


Figure 6: The effect of λ on thermal properties are plotted for H₂ (left) and LiH (right) in atomic unit. Following differences are given: classical partition functions in (A)-(B), internal energies in (C)-(D), specific heats in (E)-(F), free energies in (G)-(H), and entropies in (I)-(J). They are defined as: $\Delta Z(H_2)(\lambda_i) = [Z(\beta)]_{\lambda=0} - [Z(\beta)]_{\lambda=\lambda_i}$, where $\lambda_1, \lambda_2, \lambda_3, \lambda_4, \lambda_5$ correspond to $-0.25, 0.25, 0.75, 1$ and 1.25 . Other quantities follow accordingly.

References

1. Morse, P.M. Phys. Rev. 1929, **34**, 57.
2. Rong, Z., Kjaergaard, G., Sage, M.L. Mol. Phys. 2003, **20**, 2285.
3. Kratzer, A. Z. Phys. 1920, **3**, 289.
4. Bayrak, O., Boztosun, I., Ciftci, H. Int. J. Quant. Chem. 2007, **107**, 540.
5. Ikhdair, S.M., Sever, R. J. Math. Chem. 2009, **45**, 1137.
6. Rosen, N., Morse, P.M. Phys. Rev. 1932, **42**, 210.
7. Manning, M.F., Rosen, N. Phys. Rev. 1933, **44**, 953.
8. Chen, Z.Y., Li, M., Jia, C.S. Mod. Phys. Lett. A 2009, **24**, 1863.
9. Nasser, I., Abdelmonem. M.S., Abdel-Hady, A. Mol. Phys. 2013, **111**, 1.
10. Roy, A.K. Mod. Phys. Lett. 2014, **9**, 1450042.
11. Pöschl, G., Teller, E. Z. Phys. 1933, **83**, 143.
12. Dong, S.H., Lemus, R. Int. J. Quant. Chem. 2002, **86**, 265.
13. Atkas, M., Sever, R. J. Mol. Struct. THEOCHEM 2006, **710**, 223.
14. Linnett, J.W. Trans. Faraday Soc. 1940, **36**, 1123.
15. Hulthén, L. Ark. Mat. Astron. Fys. 1942, **28A**, 5.
16. Roy, A.K. Pramana-J. Phys. 2005, **65**, 1.
17. Jia, C.S., Diao, Y.F., Yi, L.Z., Chen, T. Int. J. Mod. Phys. A 2009, **24**, 4519.
18. Gu, X.Y., Sun, J.Q. J. Math. Phys. 2010, **51**, 022106.
19. Lippincott, E.R. J. Chem. Phys. 1953, **21**, 2070.
20. Deng, Z.H., Fan, Y.P. Shandong Univ. J. 1957, **7**, 162.

21. Oyewumi, K.J., Oluwadare, O.J., Sen, K.D., Babalola, O.A. J. Math. Chem. 2013, **51**, 976.
22. Roy, A.K. Int. J. Quant. Chem. 2014, **114**, 383.
23. Oluwadare, O.J., Oweyumi, K.J. Eur. Phys. J. Plus 2018, **133**, 422.
24. Vogt, E., Sage, D.L., Kjaergaard, H.G. Mol. Phys. 2018, **117**, 1629.
25. Boukabcha, H., Hachama, H., Diaf, A. Appl. Math. Comput. 2018, **321**, 121.
26. Tietz, T. J. Chem. Phys. 1963, **38**, 3036.
27. Hua, W. Phys. Rev. A 1990, **42**, 2524.
28. Hamzavi, M., Rajabi, A.A., Thylwe, K.E. Int. J. Quant. Chem. 2012, **112**, 2701.
29. Roy, A.K. J. Math. Chem. 2014, **52**, 1405.
30. Schiöberg, D. Mol. Phys. 1986, **59**, 1123.
31. Zavitsas, A.A. J. Am. Chem. Soc. 1991, **113**, 4755.
32. Eđrifes, H., Demirhan, D., Büyükkiliç, F. Phys. Scr. 1999, **60**, 195.
33. Sun, Y., He, S., Jia, C.S. Phys. Scr. 2013, **87**, 025301.
34. Jia, C.S., Chen, T., Yi, L.Z., Lin, R.S. J. Math. Chem. 2013, **51**, 2165.
35. Fakhri, H., Sadeghi, J. Mod. Phys. Lett. A 2004, **19**, 615.
36. Guo, J.Y., Sheng, Z.Q. Phys. Lett. A 2005, **338**, 90.
37. Ikhdaire, S.M., Sever, R. Int. J. Mod. Phys. A 2010, **25**, 3941.
38. Ikhdaire, S.M., Sever, R. J. Mol. Struct. THEOCHEM 2006, **806**, 155.
39. Oyewumi, K.J., Akinpelu, F.O., Agboola, A.D. Int. J. Theor. Phys. 2008, **47**, 1039.
40. Hajigeorgiou, P.G. J. Mol. Spect. THEOCHEM 2010, **263**, 101.
41. Mesa, A.D.S., Quesne, C., Smirnov, Y.F. J. Phys. A 1998, **31**, 321.
42. Codriansky, S., Cordero, P., Salamó, S. J. Phys. A 1999, **32**, 6287.
43. Dong, S.H., Gu, X.Y. J. Phys. Conf. Ser. 2008, **96**, 012109.
44. Zhang, L.H., Li, X.P., Jia, C.S. Int. J. Quant. Chem. 2011, **111**, 1870.

45. Zhang, L.H., Li, X.P., Jia, C.S. Phys. Scr. 2009, **80**, 035003.
46. Dong, S.H. Commun. Theor. Phys. 2011, **55**, 969.
47. Oluwadare, O.J., Oyewumi, K.J., Akoshile, C.O., Babalola, O.A. Phys. Scr. 2012, **86**, 035002.
48. Hamzavi, M., Ikhdair, S.M., Thylwe, K.E. J. Math. Chem. 2013, **51**, 227.
49. Falaye, B.J., Ikhdair, S.M., Hamzavi, M., Z. Naturforsch. 2015, **70** 85.
50. Wang, P.Q., Zhang, L.H., Jia, C.S., Liu, J.Y. J. Mol. Spect. 2012, **274**, 5.
51. Pekeris, C.L. Phys. Rev. 1934, **45**, 98.
52. Badawi, M., Bessis, N., Bessis, G. J. Phys. B 1972, **5**, L157.
53. Mustafa, O. J. Phys. B 2015, **48**, 065101.
54. Greene, R.L., Aldrich, C. Phys. Rev. A 1976, **14**, 2363.
55. Oyewumi, K.J., Falaye, B.J., Onate, C.A., Oluwadare, O.J., Yahya, W.A. Mol. Phys. 2013, **112**, 127.
56. Nikiforov, A.F., Uvarov, V.B. *Special Functions of Mathematical Physics* (Birkhäuser, Basel) (1988).
57. Berkdemir, C., Han, J. Chem. Phys. Lett. 2005, **409**, 203.
58. Tezcan, C., Sever, R. Int. J. Theor. Phys. 2009, **48**, 337.
59. Udoh, M.E., Okorie, U.S., Ngwueke, M.I., Ituen, E.E., Ikot, A.N. J. Mol. Model. 2019, **25**, 170.
60. Strelakov, M.L. Chem. Phys. Lett. 2007, **439**, 209.